J Comp Physiol A (2003) 189: 221–230
DOI 10.1007/s00359-003-0394-2

ORIGINAL PAPER

A.V. Minor · K.-E. Kaissling

Cell responses to single pheromone molecules may reflect the activation kinetics of olfactory receptor molecules

Received: 4 October 2002 / Revised: 11 December 2002 / Accepted: 9 January 2003 / Published online: 21 February 2003

Abstract Olfactory receptor cells of the silkmoth *Bombyx mori* respond to single pheromone molecules with "elementary" electrical events that appear as discrete "bumps" a few milliseconds in duration, or bursts of bumps. As revealed by simulation, one bump may result from a series of random openings of one or several ion channels, producing an average inward membrane current of 1.5 pA. The distributions of durations of bumps and of gaps between bumps in a burst can be fitted by single exponentials with time constants of 10.2 ms and 40.5 ms, respectively. The distribution of burst durations is a sum of two exponentials; the number of bumps per burst obeyed a geometric distribution (mean 3.2 bumps per burst). Accordingly the elementary events could reflect transitions among three states of the pheromone receptor molecule: the vacant receptor (state 1), the pheromone-receptor complex (state 2), and the activated complex (state 3). The calculated rate constants of the transitions between states are $k_{21} = 7.7\ s^{-1}$, $k_{23} = 16.8\ s^{-1}$, and $k_{32} = 98\ s^{-1}$.

Keywords Bombykal receptor cell · Density of receptor molecules · Dissociation constant of pheromone-receptor complex · Elementary receptor responses · Silk moth, *Bombyx mori*

Abbreviations *BAL* bombykal · *BOL* bombykol · *ERC* elementary receptor current · *ERP* elementary receptor potential · *PBP* pheromone-binding protein

A.V. Minor
Institute of Ecology and Evolution,
Leninsky prosp. 33, 117071 Moscow, Russia

K.-E. Kaissling (✉)
Max-Planck Institut fuer Verhaltensphysiologie,
Seewiesen, 82319 Starnberg, Germany
E-mail: kaissling@mpi-seewiesen.mpg.de
Tel.: +49-8157-932238
Fax: +49-8157-932209

Introduction

A typical sequence of events in sensory transduction starts with a conformational change of a G-protein-coupled receptor, and finishes with the activation of ion channels. Patch-clamp studies of channel activation provided the first example of monitoring conformational changes of a single protein molecule, the active state of which could be "seen very directly" (Colquhoun 1988). In this paper we show that the same might be possible for the conformational changes in sensory receptors. Our example is an olfactory pheromone receptor cell in the silkmoth *Bombyx mori*. The trichoid olfactory sensilla in the antenna of the male moth contain two morphologically identifiable, highly specific receptor cells that respond to (*E*,*Z*)-10,12-hexadecadien-1-ol (bombykol, BOL) and (*E*,*Z*)-10,12-hexadecadien-1-al (bombykal, BAL), respectively, which are components of the female pheromone (Butenandt et al. 1961; Kasang et al. 1978; Kaissling et al. 1978; Kumar and Keil 1996). The BAL-sensitive cell was studied in this paper.

Receptor potentials and spike discharges recorded in pheromone-sensitive cells in response to stimulation with pheromone were studied extensively in *Bombyx* and a few other silkmoth species (for review see Kaissling 1987, 2001). Combined radiometric, electrophysiological and behavioral studies (Kaissling and Priesner 1970; Kaissling 1987) showed that one pheromone molecule is sufficient to elicit a nerve impulse (spike) in a receptor cell. In brief, by using highly tritium-labeled pheromone the number of stimulus molecules adsorbed on the pheromone-sensitive hairs was determined and compared with the number of nerve impulses recorded from single olfactory hairs (sensilla trichodea). At the 20% behavioral threshold of male moths, each of the 17,000 hairs of the antenna received on average 0.04 molecules during the 1-s stimulus and produced 0.01 nerve impulses. With these numbers the probability of an individual receptor cell capturing more than one pheromone molecule is negligibly low. Furthermore, with

stimulus intensities above the behavioral threshold by a factor of up to 100, the number of nerve impulses elicited per stimulus obeyed a Poisson distribution for single random events. Spikes elicited at such low stimulus intensities are preceded by a brief bump-like potential fluctuation (Kaissling 1974, 1977; Kaissling and Thorson 1980), and some of the "bumps" may appear without spikes (Fig. 1). The olfactory bumps are mostly grouped in bursts comprising two or more bumps. Both such bursts and the solitary bumps were called elementary receptor potentials (ERPs) or currents (ERCs) when recorded under transepithelial current- or voltage-clamp conditions, respectively (Kaissling 1994; Redkozubov 2000). Each elementary event represents the initial electrical process resulting from interactions of a single pheromone molecule with a receptor molecule in the dendritic membrane of the pheromone-sensitive cell. To reveal the processes underlying the generation of elementary events, we studied the temporal parameters of bumps and bursts elicited by BAL. The analysis provides values for rate constants of transitions between three states of olfactory receptor molecules. Preliminary data were presented in Minor et al. (2001).

Materials and methods

Pupae of *B. mori* were obtained from commercial breeders and kept at room temperature. After emergence the adults were kept at 12°C until the experiments started.

Electrical activity of BAL-sensitive cells was recorded from antennal sensilla trichodea of males of *B. mori*. Due to the peculiarities of the sensillum morphology, intracellular recordings in situ from the silkmoth olfactory cells have not yet been successful. At present the technique of transepithelial tip recording from the cut hair is the only reliable method for recording receptor potentials and ERPs of the pheromone-sensitive cells in the silkmoths. Such recorded potentials correctly reflect the variations of the dendritic membrane potential (Vermeulen and Rospars 2001).

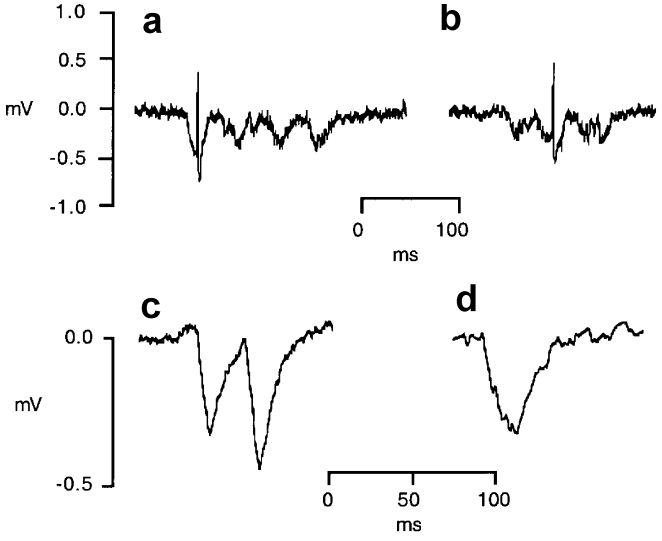

Fig. 1a–d Elementary receptor potentials of bombykal (BAL)-sensitive cells in *Bombyx* males recorded during weak stimulation. **a** Burst of four bumps. **b** Burst of three bumps; each burst with one action potential, unfiltered records from cell B. **c** A burst of two bumps. **d** A solitary bump, both at expanded scales, low-pass filtered records (500 Hz) from cell A

Transepithelial recordings were made from the tips of single sensilla trichodea located on side branches from the middle portion of isolated antennae, using glass capillaries with Ag-AgCl electrodes. Recording capillaries had a diameter at the tip of 8–10 μm and were slipped over the cut tip of one of the sensilla. The reference electrode contacting the hemolymph of the antenna was filled with hemolymph ringer solution and inserted into the antennal stem. Detailed descriptions of the preparation, electrodes, solutions and stimulation techniques were published earlier (Kaissling and Thorson 1980; Kaissling 1995; Redkozubov 2000) Transepithelial potentials under current clamp and transepithelial currents under voltage clamp were recorded with an EPC-9 patch-clamp amplifier (HEKA, Germany) and low-pass filtering (0–2 KHz, 4-pole Bessel filter).

Transepithelial voltage clamping provides conditions comparable to those of loose patch-clamp recording (Stühmer et al. 1985), where the "patch" is the outer dendritic part of the receptor cell membrane, and the transepithelial resistance, equivalent to the "seal resistance", is in the range 160–250 MΩ (Kodadová and Kaissling 1996; Redkozubov 1995). Potential responses of a few cells were recorded with a custom-made low-noise amplifier. The records were sampled off-line and analyzed by means of PULSE (HEKA) and IGOR Pro (WaveMetrics, USA) software. Additional filtering with cut-off frequency of 1 KHz or 0.5 KHz was applied before measuring the parameters of ERPs.

For long records of bump activity we applied periodic stimulation with one-second pulses every 60 s from a 10^{-3} μg BAL source. The pheromone source was a 1-cm^2 piece of filter paper placed in a glass tube of 7 mm inner diameter. During stimulation an airstream of 100 ml s^{-1} was passed through the tube and directed to the antenna positioned 5 cm behind the outlet of the tube. This stimulation maintained long-lasting ERP production with average intervals between ERPs of 1–4 s, except for shorter intervals and superimposing ERPs during the periods of stimulation. These periods plus 2 s after stimulus offset were excluded from analysis. Since the spontaneous activity of the BOL cell is on average one nerve impulse per 10 s (Kaissling and Priesner 1970) and since ERPs of the BOL cell firing nerve impulses can be recognized by the spike size, the contamination of the responses to BAL by spontaneous activity of the BOL cell can be kept negligibly small. The spontaneous activity of the BAL cell was estimated in the present experiments to be one bump per 30 s. The duration of a continuous record from one cell was usually in the range of 10–30 min. In three cells (referred to below as cells A, B, C), each record lasted more than 90 min.

During most experiments the standard ambient temperature of 17–18°C was maintained by an air conditioner. In a separate group of experiments the effects of temperature in the range 4–28°C were studied. For this purpose the warm airstream was passed through a cooling device based on a Peltier element. Temperature was controlled with a precision of 0.1°C by a miniature thermocouple positioned in the airstream close to the antennal preparation.

Computer simulation

To study the connection between the recorded time-courses of the bumps and underlying channel openings, we used a computer model of the electrical circuit of the sensillum (Fig. 2). The model circuit was based on the morphometric analysis of the sensilla trichodea in *Bombyx* (Steinbrecht 1973; Gnatzy et al. 1984) and on studies of the passive electrical properties of the sensillum (De Kramer et al. 1984; Redkozubov 1995). In the paper of Redkozubov (1995) the dendritic membrane resistance was determined. From these and morphological data the specific resistance of the dendritic membrane was found to be 7,500 Ωcm^2. The initial static model (Kaissling and Thorson 1980; Kodadová and Kaissling 1996) was extended to include

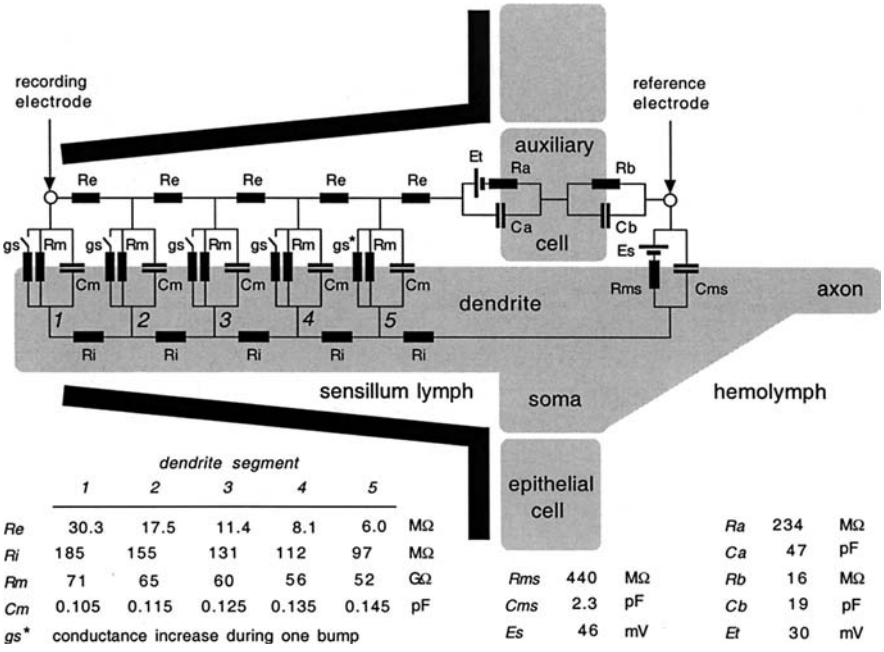

Fig. 2 Equivalent electrical circuit diagram used to simulate the bumps (modified from Kaissling and Thorson 1980). The epithelial organization of the sensillum is schematically indicated. The three auxiliary cells are combined into one compartment. Only one of the two receptor cells, the BAL receptor cell, is considered here. Two electrical paths are shown, one across the auxiliary cells and one through dendrite + soma of the receptor cell. The recording is transepithelial between sensillum lymph and hemolymph. The following values of resistances and capacitances are based on the morphology of the receptor and auxiliary cells (Steinbrecht 1973; Gnatzy et al. 1984) and on electrical measurements (De Kramer et al. 1984; Redkozubov 1995). The tapering cuticular hair (inner diameter tip 0.44 μm, base 1.22 μm) containing sensillum lymph is drawn in *black*. The hair together with the receptor cell dendrite (length after cutting the hair tip 80 μm, diameter tip 0.2 μm, base 0.3 μm) is divided into five segments. *Re* and *Ri*: resistances of external and internal medium, respectively (spec. resistance 40 Ωcm); *Rm*: resting membrane resistance of dendrite (spec. res. 7,500 Ωcm^2); *gs*: represents the conductance increase during one bump; *Rms*: resting membrane resistance at soma region (soma membrane area 230 μm^2, spec. res. 1,000 Ωcm^2); *Ra*, *Rb*: apical and basolateral membrane resistances of auxiliary cells, respectively (membrane area apical 4,700 μm^2, spec. res. 11,000 Ωcm^2, basolateral 1,900 μm^2, spec. res. 300 Ωcm^2); *Cm*, *Cms*, *Ca*, *Cb*: membrane capacitances (spec. capacitance 1 $\mu F\ cm^{-2}$). The values of membrane areas and specific resistances were adjusted to match the time-course of the bumps and the measured preparation resistance of cell A; *Es*: electromotive force (EMF) responsible for the resting potential of the soma membrane; *Et*: EMF responsible for the resting transepithelial potential (due to the electrogenic pump located in the apical membrane of auxiliary cells). The above data were used to calculate the values for each element of the circuit

membrane capacitances and transient cable effects in the dendrite. The program calculated transient potentials recorded from the hair after a single channel opening or a series of such openings in the dendritic membrane. The transient voltages were calculated by means of the Adaptive Runge-Kutta method (Press et al. 1995). The model was adjusted to a given sensillum by varying the areas of the apical and basal membranes of the auxiliary cells within the measured morphological range. Independently, specific resistances of these two membranes were also adjusted in order to keep the transepithelial resistance in the model equal to the given sensillum resistance.

Results

Two recording modes for assessing bump activity were compared on the same eight sensilla from three animals: voltage recording under transepithelial current clamp (Kaissling 1994) and current recording under transepithelial voltage clamp (Redkozubov 1995). When the transepithelial potential of the sensillum was recorded at zero current, bumps consisting of two transients (rising and falling parts) with rather sharp onsets were observed (Fig. 1). At 1 kHz bandwidth the baseline and the transients were accompanied by noise of about 30 μV r.m.s. in the short-cut hairs. The bump duration varied over a wide range, from about 1 ms to several tens of milliseconds. The briefer bumps had smaller amplitudes. A typical bump had a duration of at least 5 ms and an amplitude of 200–400 μV. When the transepithelial potential was clamped at the resting value, current bumps were recorded with typical amplitude of 1–2 pA for longer bumps. They showed faster transients and had more rectangular shapes than in current clamp. We had expected the transepithelial voltage clamp to increase the amplitudes of brief bumps, but the dominant factor proved to be the relatively large current noise (0.5–0.6 pA r.m.s. at 1 kHz bandwidth). Even with additional filtering, the signal-to-noise ratio under voltage clamp was much worse than under current clamp. Therefore recording in the current-clamp mode was chosen for the measurements of ERP parameters.

To understand the unexpected disadvantage of transepithelial voltage clamp, we considered a simplified equivalent electrical circuit of the sensillum, which consisted of the resistance and capacitance of the apical membranes of auxiliary cells, (R_a and C_a in parallel and a serial resistance $R_b + R_e$ (Fig. 2). R_e was estimated as 25.5 MΩ for the hairs cut to about 50% of the initial length (the resistance of the three basal hair segments

shown in Fig. 2). Theoretical r.m.s. values of the voltage and current thermal noise at 18°C for this circuit were calculated by means of standard techniques (Bennett 1960). The signal was calculated as a convolution of the response function of the circuit to a rectangular 2-pA current pulse of variable duration, and that of the low-pass filter. As revealed by these calculations, at 1-kHz frequency band in the bump-duration range between 5 ms and 30 ms the transepithelial voltage-clamp recording mode was expected to show 2–4.5 times lower signal-to-noise ratio than the current clamp mode.

The responses of two especially long lasting BAL receptor cells (cells A and B) were evaluated, with 452 and 375 ERPs, respectively. The values found for cell B are given in brackets. The measured parameters are shown in Fig. 3. The beginning of the bump was defined as the moment of transition from the baseline to the rising part of the bump (drawn downward). The end of the bump was defined as the moment of transition from the rising to falling part of the bump (drawn upward). The intervals between bursts (d_1), the intervals between bumps in a burst (d_2), the bump durations (d_3), and the burst durations (d_4) were measured as intervals between the beginnings and ends of the respective bumps in a series of ERPs. In bumps with nerve impulses the falling part of the bump is merged with the rising part of the spike. This creates an error of a few milliseconds mostly affecting the measurements of the bump duration. For this reason the parameter d_3 was measured in the bumps that were not accompanied by spikes.

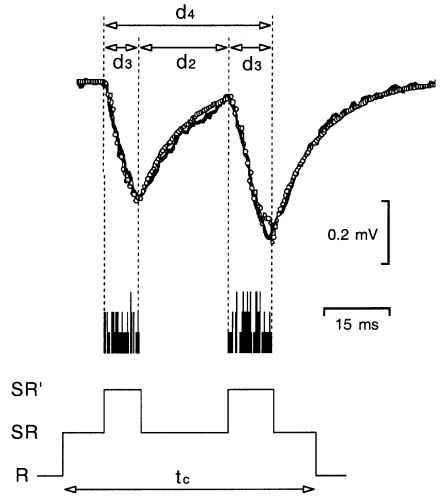

Fig. 3 Model simulation of an elementary receptor potential (ERP). *Top traces*: same burst as in Fig. 1c (*black trace*) and its simulation (*thin trace with open symbols*). The simulation is a response of the model electric circuit (Fig. 2) to two series of random openings of three ion channels, 56 pS each, with mean opening durations of 1.2 ms and mean open probability of 0.24 as recorded in Zufall and Hatt (1991). *Middle*: columns represent the pattern of openings of three channels underlying the simulated bumps. *Bottom trace*: pattern of transients between three states R, SR, and SR' in a simple model of agonist (S)-receptor (R) interaction (see Discussion). The measured variables of bump activity shown are the gap duration (d_2), bump duration (d_3), and burst duration (d_4). The lifetime of the complex is t_c

In the range of stimulus intensities used in our experiments, the intervals between bursts (d_1) were on average 25–100 times longer than the gaps within bursts; thus, the probability of overlapping of bursts was very small. The mean values of the variables d_2, d_3, d_4, and n are independent of stimulus intensity. Notably, all measured random variables obeyed simple distribution laws. The histograms of d_1 (Fig. 4), d_2, and d_3 (Fig. 5a, b) are well fitted by single exponential functions; the distribution of the number of bumps in a burst (n) (Fig. 5c) is fitted by a geometric distribution (an exponential with integer argument) $G(n)$. The number of events observed at $n=1$ (not shown) was higher than was expected for the "one-bump bursts". This can be explained by spontaneous solitary bump activity, which was observed in the absence of stimulation.

The mean values of d_2, and d_3 are represented by the time constants of the exponential curves (Fig. 5a, b), with the values for cell A of $D_2 = 40.5$ ms (cell B: 35.6 ms) and $D_3 = 10.2$ ms (cell B: 10.1 ms). The value of D_3 was determined for five cells (including A and B) as 9.8 ± 0.61 ms (mean ± SEM). The probability p of appearance of an additional bump in a burst was found as

$$p = \frac{G(n+1)}{G(n)} \tag{1}$$

The measured value of p was 0.689 (cell B: 0.685) (Fig. 5c). All of these values show little variation between the two cells. The mean number of bumps per burst was calculated as

$$N = \frac{1}{1-p} = 3.2(\text{cell B: } 3.2). \tag{2}$$

The distribution of the measured burst duration d_4 (Fig. 5d) was fitted with a sum of two exponentials with the time constants D_{41} and D_{42} and the weighting factors w_1 and w_2, respectively (Table 1). The mean burst duration D_4, calculated from the double-exponential distribution of d_4, was

$$D_4 = \frac{w_1 \cdot D_{42}^2 + w_2 \cdot D_{42}^2}{w_1 \cdot D_{41} + w_2 \cdot D_{42}} = 118 \text{ ms}(\text{cell B: } 70\text{ms}). \tag{3}$$

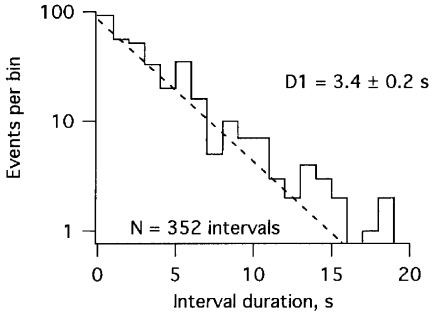

Fig. 4 Distribution of intervals (d_1) between ERPs recorded from a single receptor cell (cell B), exponential fitting. The average interval is represented by the time constant D_1

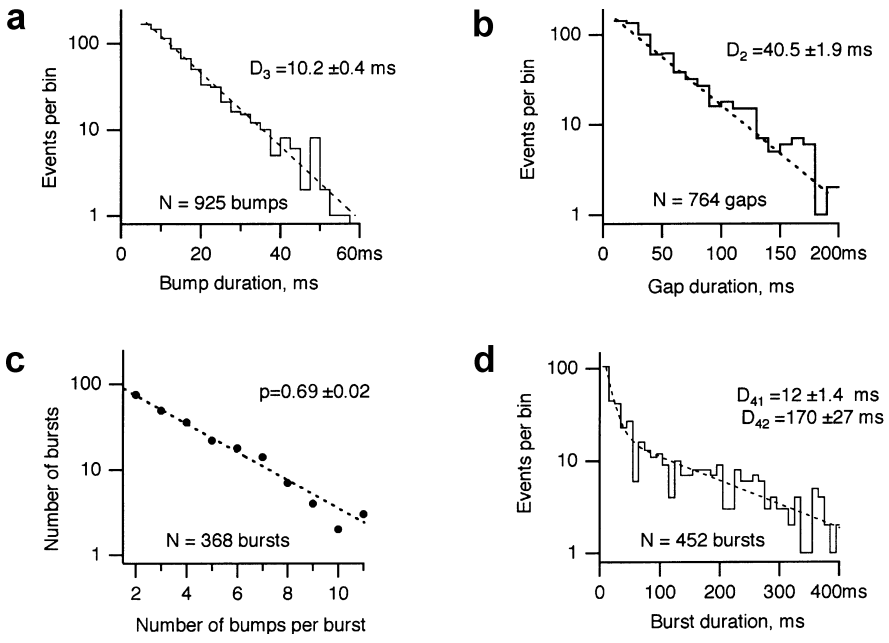

Fig. 5a–d Stochastic properties of ERPs (cell A). **a** Distribution of bump durations (d_3). The histogram is fitted with a single exponential. The time constant D_3 represents the average bump duration (±SD). **b** Distribution of gap durations (d_2) in bursts (time constant D_2, representing the average gap duration). **c** Distribution of the number of bumps in a burst (n). The diagram shows a geometric distribution. The characteristic parameter $p = 0.69$ represents the probability of occurrence of an additional bump in a burst after one or more bumps appeared. **d** Distribution of burst durations. Double-exponential fitting gives the fast and slow time constants D_{41} and D_{42} with the weighting factors w_1 and w_2, respectively

Table 1 Two ways of determining burst parameters, values of cell A (cell B). First column: parameters of distribution of burst duration d_4. Second column: predictions assuming a three-state model and based on measured distributions of d_2,d_3, and n. Third column: average values based on the directly measured distribution of d_4 (Fig. 5d)

Parameters	Predictions	Direct measurements
D_4	$\frac{D_3+p\cdot D_2}{1-p} = 123$ ms(109 ms)	118 ms (70 ms)
D_{41}	$\frac{2\cdot D_2\cdot D_3}{D2+D3+Z} = 9$ ms(8 ms)	12 ms (19 ms)
w_1	$\frac{Z-D_3+D_2}{2\cdot Z} = 0.83(0.82)$	0.87 (0.91)
D_{42}	$\frac{2\cdot D_2\cdot D_3}{D_2+D_3-Z} = 154$ ms(137 ms)	170 ms (140 ms)
w_2	$\frac{Z+D_3-D_2}{2\cdot Z} = 0.17(0.18)$	0.14 (0.09)

$Z = \sqrt{(D_2+D_3)^2 - 4\cdot(1-p)\cdot D_2\cdot D_3}$

$p = (N-1)/N$

Temperature dependence of bump duration

When the temperature of the preparation was varied, the recorded ERP showed dramatic changes in the bump durations and amplitudes (Fig. 6). At lower temperature the amplitudes of bumps and spikes increased. This was explained by the increase of resting membrane resistances of the receptor and auxiliary cells (Kodadová and Kaissling 1996). During a long-lasting recording of bump activity in cell C marked changes of bump duration distribution, reflecting the increase of the bump mean duration D_3, were also observed. Cooling from 19.5°C to 4.5°C resulted in an almost threefold increase of the bump mean duration (Fig. 6). In 5 cells the average data for the temperature effect on D_3 gives $Q_{10} = 1.9$ (Fig. 7).

Simulation of bumps

The time course of a recorded bump could be simulated by a single opening of an ion channel in the dendritic membrane, for a period equal to the bump duration. According to the static circuit model the conductance of a single channel would be 22.5 pS to produce a bump current of 1.5 pA, in agreement with Fig. 2 in Redkozubov (2000). The corresponding voltage amplitude of the bump is 0.4 mV. Instead of a single comparatively long opening – atypical for ion channels – a series of random openings can be applied for the same period in order to simulate a bump. In this case the channels are thought to be activated by a pulse-like increase of ligand concentration, e.g., of second-messenger molecules released by the activation of the receptor molecule. For the simulation we used channels with an opening duration of 0.12 ms, a mean open probability during activation of 0.24, and a conductance of 56 pS such as observed in pheromone-activated channels in a different silk moth *Antheraea polyphemus* (Zufall and Hatt 1991). Simulated responses using three or four channels closely fit a given recorded bump (Fig. 3). When 750 bumps were simulated using one to five ion channels activated per bump, the distribution of a mixture of all bump amplitudes was broad and obviously non-Gaussian, like that found experimentally (Redkozubov 2000).

Discussion

The generation of bumps

So far there is no quantitative understanding of how olfactory signals are transduced in insects (Zufall and Hatt 1991; Kaissling and Boekhoff 1993; Stengl et al.

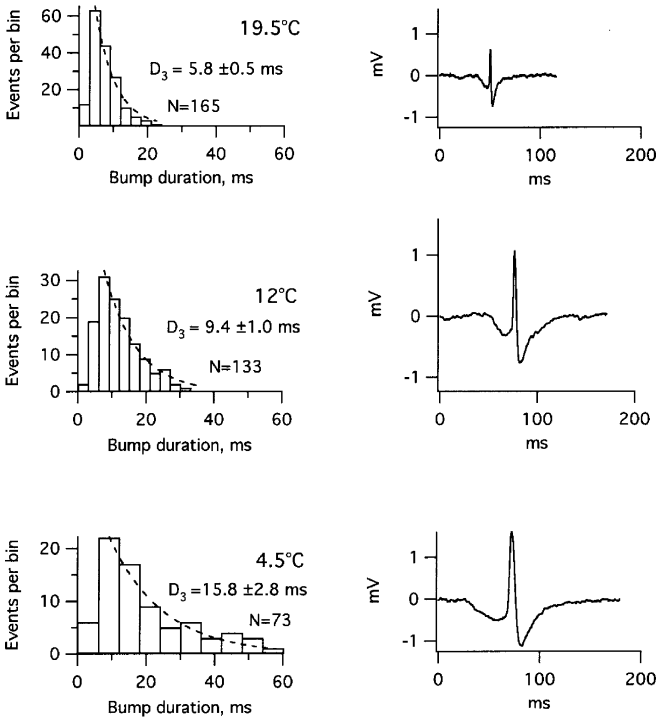

Fig. 6 Bump duration at different temperatures, recorded from the same BAL cell. Exponential fitting of the distributions (time constant D_3, representing average bump duration). *Right-hand panels*: examples of bumps eliciting one spike

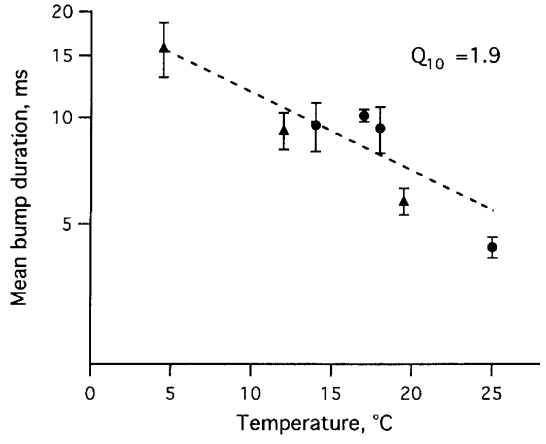

Fig. 7 Mean bump duration (D_3) as a function of temperature. Values of D_3 (±SEM) from five cells. *Triangles*: data from Fig. 6; *dashed line*: exponential fit corresponding to $Q_{10}=1.9$

1992, 1999; Krieger and Breer 1999). Recently G protein-coupled olfactory receptors were discovered in *Drosophila* (Vosshall et al. 1999; Clyne et al. 1999). There is evidence that G protein, phospholipase C and protein kinase C are components of the intracellular olfactory transduction system in the moths *Manduca sexta* (Stengl et al. 1992, 1999) and *A. polyphemus* (Laue et al. 1997; Maida et al. 2000; Kaissling 1996). Rapid concentration changes of a hypothetical messenger seem possible since within sensory dendrites 0.1–0.5 μm in diameter the diffusion times are very short. Note that a sharp decrease of messenger concentration would require a fast removal of the messenger.

Models of generation of bumps and bursts

Several models of the generation of the observed elementary responses by a single pheromone molecule may be considered. In the first type of model the pheromone molecule interacts with several receptor molecules in succession. The burst duration could represent a dwell time during which the stimulus molecule remains in the vicinity of the receptor cell membrane (Berg and Purcell 1977). Each bump reflects the activation of a single receptor molecule and the induced increase of second messenger ("agonist") concentration. The burst of bumps would terminate with the pheromone molecule leaving the receptor area (due to rebinding to pheromone-binding protein (PBP) or degradation by an enzyme). Such a mechanism seems relatively unlikely since it includes an additional state, in which the pheromone is bound to the PBP (or an enzyme), and would lead to distributions of bumps and gaps different from those observed here.

In the second type of model the pheromone molecule interacts with only a single receptor molecule. Here we discuss three models which are distinguished by their temporal characteristics (Fig. 8), but may produce similar patterns of bursts and bumps. They all satisfy the main demand that one pheromone molecule initiates a single bump or one burst of bumps. In all of these models the burst persists as long as the receptor molecule is occupied by the stimulus molecule, and a bump is produced by a group of single channel openings such as observed by Zufall and Hatt (1991).

Model 1

The elementary event reflects the pattern of receptor activation and of the respective agonist concentration. During each activation the latter concentration is elevated. One or several channels are occupied by agonists for time intervals shorter than the time of a single receptor activation. During its occupation a given channel may produce several openings.

Model 2

After occupation by the pheromone the receptor is activated only once. During the period of elevated agonist concentration, a channel binds an agonist molecule one or several times. The bump duration reflects the occupation of the channel by the agonist. The onset of bumps and the gap duration are not controlled by the receptor molecule. The bumps occur at random as long as the agonist concentration is elevated. This model works only with one channel controlled by the receptor molecule,

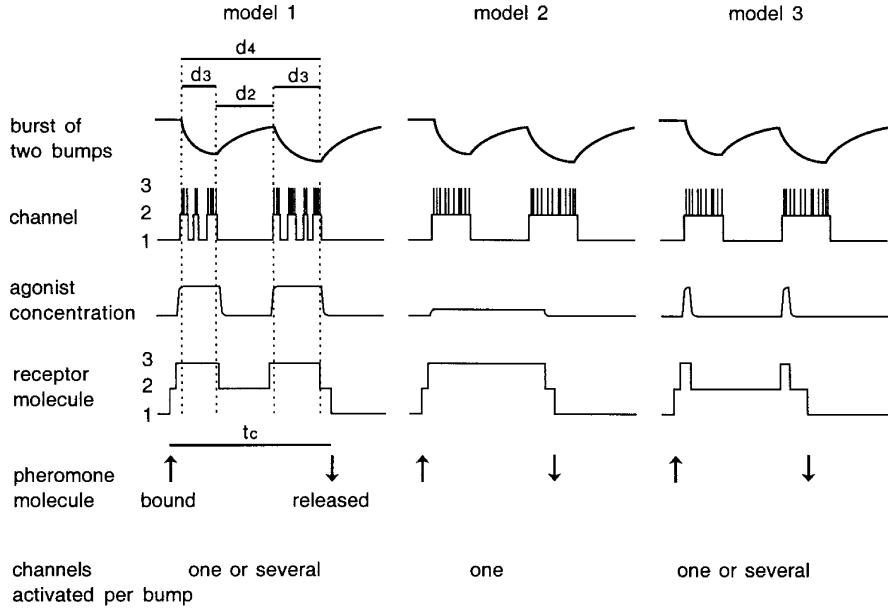

Fig. 8 Schematic representation of three models of ERP generation discussed. Measured burst parameters are d_2 (gap duration), d_3 (bump duration), and d_4 (burst duration). It is assumed that a single pheromone molecule occupies a receptor molecule (receptor state $1 \rightarrow 2$) for a time interval t_c. If the receptor molecule is activated (receptor state $2 \rightarrow 3$) an agonist (second messenger) concentration is produced which lasts for the activation period. Agonist molecules bind to channel molecules (channel state $1 \rightarrow 2$) which may be opened several times during one occupation event (channel state $2 \rightarrow 3$). *Model 1*: burst of bumps reflects the pattern of receptor occupation and activation. *Model 2*: the burst duration depends on the occupation of the receptor by the pheromone whereas bump and gap durations reflect the channel kinetics. Only one channel may be activated per bump since the pattern of bumps and gaps would be blurred with several such channels of random kinetics. *Model 3*: the burst duration depends on the occupation by the pheromone, the receptor activation triggers the onset of bumps. The bump duration reflects the occupation of the channels by the agonists

since with several channels it could not produce the observed pattern of bumps and gaps.

Model 3

The receptor activation lasts for a time shorter than the bump duration, and triggers the onset of each bump as in model 1. The bump duration, however, reflects the channel occupation by the agonist as in model 2.

Of the three models of interaction with a single receptor molecule, models 2 and 3 seem to be inconsistent with electrophysiological responses to some pheromone analogues (Kaissling 1974, 1977, 1994; Kaissling and Thorson 1980). Of these analogues 100- to 1,000-fold higher concentrations than of the pheromone were required to obtain the same overall amplitude of the receptor potential. In contrast to the pheromone, these compounds did not elicit detectable ERPs or, at higher stimulus concentrations, a depolarization with a time-course fluctuating due to superimposed bumps. Instead they produced a smooth depolarization, indicating superimposition of many but smaller elementary responses. The latter may be produced by bumps with a duration so short that the single bumps are invisible due to the capacitances of the sensillum circuit. Since these analogs most likely act on the pheromone receptor molecules, and not on later stages of the transduction cascade, the receptor molecules are probably the controlling molecules responsible for bump and burst parameters as in model 1. The reduced effectiveness of the analogues may not only be due to a lower probability of binding to and activation of a receptor molecule but also to a shorter duration of the activated state leading to shorter bumps (Kaissling 2001). The alternative possibility of separate receptor molecules for pheromone analogs seems unlikely for these highly specific cells tuned to the female pheromone components.

There exist other arguments favoring model 1 based on the temporal characteristics of the various models. In model 1 a common three-state mechanism (see below) allows certain relations to be predicted between the parameters of burst and bump activity, as shown in Table 1 (see below). These relations are not expected in models 2 and 3, where the temporal pattern of the elementary responses is controlled by two different and independent mechanisms, the receptor and channel activations. In this respect our experimental data support model 1. One consequence of two different mechanisms, responsible for bump and burst generation in model 3, would be the possibility of overlapping bumps within a burst. The overlapping may happen if the receptor is activated before the channel occupation has been terminated. Such overlapping, which is impossible in model 1, would result in modified distribution curves for the bump and burst parameters, which were not observed in the experiments. Another argument is that in model 1 the distributions and mean values of d_2, d_3, and d_4 do not depend on stimulus concentration. In contrast, in model 2 the gap duration (d_2) depends on

the stimulus (and hence agonist) concentration, and is expected to be shorter at stronger stimulation. This is inconsistent with our experimental data, which did not show such dependence.

We remain with model 1, in which the transients between states of the receptor molecule govern the temporal pattern of the ERPs. This implies that the processes downstream of the receptors are faster than the receptor processes.

The three-state receptor model of elementary responses

The distribution parameters of bursts and bumps satisfy a simple three-state mechanism of ligand-receptor interaction such as described for ligand-gated channels (Del Castillo and Katz 1957; Colquhoun and Hawkes 1981, 1982). According to this mechanism we hypothesize that the generation of a burst of bumps is controlled by transitions among three states of the receptor molecule R interacting with the stimulus molecule S (model 1, see above). The three states are the vacant R (state 1), a complex SR of S bound to R (state 2), and an activated complex (SR', state 3), which initiates the cell depolarization either directly or via relatively fast processes downstream in the transduction chain. Random transitions are possible between states 1 and 2 and between states 2 and 3, but not between states 1 and 3. They are considered as Poisson processes determined by the rate coefficients r_{12}, r_{21}, r_{23}, and r_{32}, respectively, which specify the mean numbers of transitions of a molecule R per unit time. The rate coefficients r_{21}, r_{23}, and r_{32} coincide with the rate constants of the corresponding molecular reactions: $r_{21}=k_{21}$, $r_{23}=k_{23}$, $r_{32}=k_{32}$. Only the coefficient r_{12} depends on the stimulus concentration [S]: it is the product of [S] and the rate constant k_{12}. We suggest that the transitions between states 2 and 3 can be observed as onsets and offsets of the bumps. An observed burst d_4 begins with the first and ends with the last bump within the lifetime T_c of the complex SR, and is shorter than the latter (see Fig. 3, bottom trace). The transitions between states 1 and 2 are not observable.

In the three-state model the distributions of d_2, d_3, d_4, and n are fully determined by the three rate constants r_{21}, r_{23}, and r_{32}, according to the following relationships:

$$D_2=\frac{1}{r_{21}+r_{23}} \quad D_3=\frac{1}{r_{32}} \quad N=\frac{r_{21}+r_{23}}{r_{21}} \quad p=\frac{r_{23}}{r_{21}+r_{23}} \tag{4}$$

The three rate constants can be calculated from the parameters of the distributions found experimentally:

$$r_{21}=\frac{1-p}{D_2}=7.7\,s^{-1}\left(\text{cell B}: 8.8\,s^{-1}\right); \tag{5}$$

$$r_{23}=\frac{p}{D_2}=16.8\,s^{-1}\left(19.2\,s^{-1}\right); \tag{6}$$

$$r_{32}=\frac{1}{D_3}=98\,s^{-1}\left(99\,s^{-1}\right). \tag{7}$$

The temperature effects on D_3 suggest an associated decrease of the corresponding rate constant r_{32}. The three-state model implies certain relations between the parameters p, D_2, D_3 and the burst parameters obtained from measuring d_4 (D_4, D_{41}, w_1, D_{42}, and w_2). This allows two ways of determining the burst parameters as shown in Table 1. The calculated and experimental values (second and third column of Table 1, respectively) match fairly well in cell A. In cell B the match is less good for the values of D_4, D_{41}, and w_2. The three-state model also allows estimation of the mean lifetime of the stimulus-receptor complex (T_c), which is not directly observable

$$T_c=N\cdot D_2+(N-1)\cdot D_3 =\frac{D_2+p\cdot D_3}{1-p}=153\,\text{ms}(\text{cell B}: 135\text{ ms}). \tag{8}$$

where N is the mean number of bumps per burst, whereas the mean number of bumps per complex formation is $N-1$. With

$$D_4=N\cdot D_3+(N-1)\cdot D_2=\frac{D_3+p\cdot D_2}{1-p} =123\text{ ms}(\text{cell B}: 109\,\text{ms}) \tag{9}$$

one finds $T_c=D_4+D_2-D_3$. The mean lifetime (T_c) expressed using the rate constants r_{21}, r_{23}, and r_{32} is

$$T_c=\frac{1}{r_{21}}+\frac{r_{23}}{r_{12}\cdot r_{32}} \tag{10}$$

It should be noted that in Equation 13 in Kaissling (2001) the term in brackets equivalent to T_c/p has been inaccurately denoted as a dwelling time of the stimulus-receptor complex. The term p (see above) represents the fraction of stimulus-receptor complexes leading to activation of the receptor (state 3) at least once, a prerequisite for firing a nerve impulse.

The types of distributions of d_2, d_3, d_4, and n—together with the match between the values found from the equations for D_{41}, w_1, D_{42}, w_2, and D_4 and the values found from direct experimental measurement of d_4 (Table 1)—are compatible with a simple three-state mechanism in which all three states relate to a single controlling molecule, the pheromone receptor – as described in model 1 Fig. 8.

It should be noted that for this analysis it is not important whether the stimulus S represents the pheromone as a free molecule or a complex of pheromone and PBP. There is some evidence for the latter in *Antheraea polyphemus* (Kaissling 2001) and in *Lymantria dispar* (Kowcun et al. 2001), while in *B. mori* the complex pheromone-PBP might dissociate immediately before the interaction of pheromone and receptor takes place (Wojtasek and Leal 1999; Horst et al. 2001).

Concluding remarks

In conclusion we propose that the ERPs reflect the activation kinetics of the receptor molecules. While binding a stimulus molecule the receptor molecule may once or several times switch to the activated state. Each receptor activation produces – possibly via rapid second messenger release and transport – a bump by openings of a small number of ion channels of the type described by Zufall and Hatt (1991).

The proposal of a simple three-state model underlying the elementary responses in the silkmoth is a working simplification. Tentatively, we can consider the conformational transitions between three states of the pheromone receptor, R, SR, and SR', as the main processes that are reflected in the temporal pattern of ERPs, visible either through the direct gating of an ion channel or, more likely, by means of a fast secondary receptor-to-channels signaling. Elementary responses to single pheromone molecules found in *Bombyx* and a few other silkmoth species seem a promising tool for studying the transduction kinetics in olfactory receptor cells. The rate constants r_{21}, r_{23} and r_{32} determined here have been used to estimate the dissociation constant of the stimulus-receptor complex and the number of receptor molecules per receptor cell (Kaissling 2001; Kaissling and Minor 2002. This will be pursued in a seperate publication.

Acknowledgements We thank J. Thorson, Oxford, for computer programs and critical comments, B. Lindemann for helpful discussion, and A. Biederman-Thorson for help in preparing the manuscript. Valuable suggestions were given by R. A. Steinbrecht, B. Pophof, W. M. van der Goes van Naters, and G. Ziegelberger. This work was partially supported by RFBR grant no. 01-04-48035.

References

Bennett W (1960) Electrical noise. McGraw-Hill, New York

Berg HC, Purcell EM (1977) Physics of chemoreception. Biophys J 20:193–219

Butenandt A, Beckmann R, Stamm D (1961) Über den Sexuallockstoff des Seidenspinners. II. Konstitution und Konfiguration des Bombykols. Hoppe Seylers Z Physiol Chemie 324:84–87

Clyne PJ, Warr CG, Freeman MR, Lessing D, Kim J, Carlson JR (1999) A novel family of divergent seven-transmembrane proteins: candidate odorant receptors in *Drosophila*. Neuron 22:327–338

Colquhoun D (1988) Binding, gating, affinity and efficacy: the interpretation of structure-activity relationships for agonists and the effects of mutating receptors. Br J Pharmacol 125:924–947

Colquhoun D, Hawkes AG (1981) On the stochastic properties of single ion channels Proc R Soc Lond Ser B 211:205–235

Colquhoun D, Hawkes AG (1982) On the stochastic properties of bursts of single ion channel openings and of clusters of bursts. Philos Trans R Soc Lond B 300:1–59

De Kramer JJ, Kaissling K-E, Keil T (1984) Passive electrical properties of insect olfactory sensilla may produce the biphasic shape of spikes. Chem Senses 8:289–295

Del Castillo J, Katz B (1957) Interaction at end-plate receptors between different choline derivatives. Proc R Soc Lond Ser B 146:369–381

Gnatzy W, Mohren W, Steinbrecht RA (1984) Pheromone receptors in *Bombyx mori* and *Antheraea pernyi*. II. Morphometric analysis. Cell Tissue Res 235:35–42

Horst R, Damberger F, Luginbühl P, Güntert P, Peng G, Nikonova L, Leal W, Wüthrich K (2001) NMR structure reveals intramolecular regulation mechanism for pheromone binding and release. Proc Natl Acad Sci USA 98:14374–14379

Kaissling K-E (1974) Sensory transduction in insect olfactory receptors. In: Jaenicke L (ed) Biochemistry of sensory functions. 25th Mosbacher Colloquium der Gesellschaft für Biologische Chemie. Biochemistry of sensory functions. Springer, Berlin Heidelberg New York, pp 243–272

Kaissling K-E (1977) Structures of odour molecules and multiple activities of receptor cells. In: Le Magnen J, MacLeod P (eds) Int Symp Olfaction and Taste VI. Information Retrieval, London, pp 9–16

Kaissling K-E (1987) In: Colbow K (ed) R.H. Wright lectures on insect olfaction. Simon Fraser University, Burnaby, Canada

Kaissling K-E (1994) Elementary receptor potentials of insect olfactory cells. In: Kurihara K, Suzuki N, Ogawa H (eds) Int Symp Olfaction Taste XI, Springer, Tokyo, pp 812–815

Kaissling K-E (1995) Single unit and electroantennogram recordings in insect olfactory organs. In: Spielman AI, Brand JG (eds) Experimental cell biology of taste and olfaction. Current techniques and protocols. RCC, Boca Raton, pp 361–377

Kaissling K-E (1996) Peripheral mechanisms of pheromone reception in moths. Chem Senses 21:257–268

Kaissling K-E (2001) Olfactory perireceptor and receptor events in moths: a kinetic model. Chem Senses 26:125–150

Kaissling K-E, Boekhoff I (1993) Transduction and intracellular messengers in pheromone receptor cells of the moth *Antheraea polyphemus*. In: Wiese K, Gribakin FG, Popov AV, Renninger G (eds) Sensory systems of arthropods. Birkhäuser, Basel, pp 489–502

Kaissling K-E, Minor AV (2002) Pheromone receptor cells: density of receptor molecules and dissociation constant of the pheromone-receptor complex. Chem Senses (in press)

Kaissling K-E, Priesner E (1970) Die Riechschwelle des Seidenspinners. Naturwissenschaften 57:23–28

Kaissling K-E, Thorson J (1980) Insect olfactory sensilla: structural, chemical and electrical aspects of the functional organisation. In: Sattelle DB, Hall LM, Hildebrand JG (eds) Receptors for transmitters, hormones and pheromones in insects. Elsevier, Amsterdam, pp 261–282

Kaissling K-E, Kasang G, Bestmann HJ, Stransky W, Vostrowsky O (1978) A new pheromone of the silkworm moth *Bombyx mori*. Sensory pathway and behavioral Effect. Naturwissenschaften 65:382–384

Kasang G, Kaissling K-E, Vostrowski O, Bestmann HJ (1978) Bobykal, A second pheromone component of the silkworm moth *Bombyx mori* L. (in English). Angewandte Chemie Int Ed 17:60

Kodadová B, Kaissling K-E (1996) Effect of temperature on silkmoth olfactory responses to pheromone can be simulated by modulation of resting cell resistances. J Comp Physiol A 179:15–27

Kowcun A, Honson N, Plettner E (2001) Olfaction in the gypsy moth *Lymantria dispar*: Effect of pH, ionic strength and reductants on pheromone transport by pheromone binding proteins. J Biol Chem 276:44770–44776

Krieger J, Breer H (1999) Olfactory reception in invertebrates. Science 286:720–723

Kumar GL, Keil TA (1996) Pheromone stimulation induces cytoskeletal changes in olfactory dendrites of male silkmoths (Lepidoptera, Saturniidae, Bombycidae). Naturwissenschaften 83:476–478

Laue M, Maida R, Redkozubov A (1997) G-protein activation, identification and immunolocalization in pheromone-sensitive sensilla trichodea of moths. Cell Tissue Res 288:149–158

Maida R, Redkozubov A, Ziegelberger G (2000) Identification of PLCβ and PKC in pheromone receptor neurons of *Antheraea polyphemus*. Neuroreport 11:1773–1776

Minor AV, Kaissling K-E, Thorson J (2001) Elementary electrical events in moth olfactory cells: a three-state model of the receptor mechanism suffices. Chem Senses 26:792

Press WH, Teukolsky SA, Vetterling WT, Flannery BP (1995) Numerical recipes in C. The art of scientific computing, 2nd edn. Cambridge University Press, Cambridge

Redkozubov A (1995) High electrical resistance of the bombykol cell in an olfactory sensillum of *Bombyx mori*: Voltage- and current-clamp analysis. J Insect Physiol 41:451–455

Redkozubov A (2000) Elementary receptor currents elicited by a single pheromone molecule exhibit quantal composition. Pflugers Arch 440:896–901

Steinbrecht RA (1973) Der Feinbau olfaktorischer Sensillen des Seidenspinners (Insecta, Lepidoptera). Z Zellforsch 139:533–565

Stengl M, Hatt H, Breer H (1992) Peripheral processes in insect olfaction. Annu Rev Physiol 54:665–681

Stengl M, Ziegelberger G, Boekhoff I, and Krieger J (1999) Perireceptor events and transduction mechanisms in insect olfaction. In Hansson BS (ed) Insect olfaction. Springer, Berlin Heidelberg New York, 49–66

Stühmer W, Roberts WM, Almers W (1985) The loose patch clamp. In: Sakmann B, Neher E (eds) Single-channel recording. Plenum Press, New York, pp 123–132

Vermeulen A, Rospars JP (2001) Membrane potential and its electrode-recorded counterpart in an electrical model of an olfactory sensillum. Eur Biophys J 29:587–596

Vosshall LB, Amrein H, Morozov PS, Rzhetsky A, Axel R (1999) A spatial map of olfactory receptor expression in *Drosophila* antenna. Cell 96:725–736

Wojtasek H, Leal WS (1999) Conformational change in the pheromone-binding protein from *Bombyx mori* induced by pH and by interaction with membranes. J Biol Chem 274:253–308

Zufall F, Hatt H (1991) Dual activation of sex pheromone-dependent ion channels from insect olfactory dendrites by protein kinase C activators and cyclic GMP. Proc Natl Acad Sci USA 88:8520–8524